The ISME Journal (2010) 4, 1180–1192

www.nature.com/ismej

ORIGINAL ARTICLE

Significant CO_2 fixation by small prymnesiophytes in the subtropical and tropical northeast Atlantic Ocean

Ludwig Jardillier[1,3], Mikhail V Zubkov[2], John Pearman[1] and David J Scanlan[1]
[1]*Department of Biological Sciences, University of Warwick, Coventry, UK and* [2]*National Oceanography Centre, Southampton, Hampshire, UK*

Global estimates indicate the oceans are responsible for approximately half of the carbon dioxide fixed on Earth. Organisms $\leqslant 5\,\mu m$ in size dominate open ocean phytoplankton communities in terms of abundance and CO_2 fixation, with the cyanobacterial genera *Prochlorococcus* and *Synechococcus* numerically the most abundant and more extensively studied compared with small eukaryotes. However, the contribution of specific taxonomic groups to marine CO_2 fixation is still poorly known. In this study, we show that among the phytoplankton, small eukaryotes contribute significantly to CO_2 fixation (44%) because of their larger cell volume and thereby higher cell-specific CO_2 fixation rates. Within the eukaryotes, two groups, herein called Euk-A and Euk-B, were distinguished based on their flow cytometric signature. Euk-A, the most abundant group, contained cells $1.8 \pm 0.1\,\mu m$ in size while Euk-B was the least abundant but cells were larger ($2.8 \pm 0.2\,\mu m$). The Euk-B group comprising prymnesiophytes ($73 \pm 13\%$) belonging largely to lineages with no close cultured counterparts accounted for up to 38% of the total primary production in the subtropical and tropical northeast Atlantic Ocean, suggesting a key role of this group in oceanic CO_2 fixation.
The ISME Journal (2010) **4,** 1180–1192; doi:10.1038/ismej.2010.36; published online 15 April 2010
Subject Category: geomicrobiology and microbial contributions to geochemical cycles
Keywords: CO_2 fixation; primary production; prymnesiophytes; chrysophytes

Introduction

Looking inside the phytoplankton 'black box' to determine the distribution of carbon biomass and group-specific primary production is fundamental to understanding the roles of these groups in the global carbon cycle. The contribution of different phytoplankton communities to primary production has been extensively studied using size fractionation approaches (Teira *et al.*, 2005; Pérez *et al.*, 2006), and revealed a major role of the smallest phytoplankton (<2–$5\,\mu m$) in the open ocean. Direct flow cytometric sorting of these smallest picoplankton cells coupled with radioactive tracer experiments have shown that although cyanobacteria dominated carbon fixation into biomass in the open ocean, nevertheless eukaryotic cells contributed significantly in spite of their lower abundance (Li, 1994). Subsequent studies conducted in both coastal (Worden *et al.*, 2004) and open ocean waters (Goericke, 1998; Grob *et al.*, 2007), which did not involve cell sorting, supported Li's observations. Moreover, studies based on size-fractionated pigment analysis also suggest a wide distribution of these small photosynthetic eukaryotes (Latasa and Bidigare, 1998; Wright *et al.*, 2009). Recent progress using molecular approaches has begun to reveal their diversity (Moon-van der Staay *et al.*, 2000; Díez *et al.*, 2001; Vaulot *et al.*, 2008; Worden and Not, 2008) showing a dominance of prymnesiophytes, pelagophytes and prasinophytes in marine environments (for example, see Moon–van der Staay *et al.*, 2001; Romari and Vaulot, 2004; Not *et al.*, 2004; Fuller *et al.*, 2006a, b; Viprey *et al.*, 2008; Liu *et al.*, 2009) and lately of chrysophytes (Fuller *et al.*, 2006b; McDonald *et al.*, 2007; Lepère *et al.*, 2009). However, we still have a poor understanding of the phylogenetic affiliation of the smallest cells (for example, see Liu *et al.*, 2010), and particularly in directly linking taxonomic identity with ^{14}C primary production measurements. In this study, to determine the precise contributions of different phytoplankton groups to CO_2 fixation into biomass in the subtropical and tropical northeast Atlantic Ocean, we used a modified $NaH^{14}CO_3$ radiotracer incubation flow cytometric sorting approach (Li, 1994) on board ship with natural communities sampled in surface waters (between 5 and 20 m) in which the majority of CO_2 fixation is thought to occur

Correspondence: DJ Scanlan, Department of Biological Sciences, University of Warwick, Gibbet Hill Road, Coventry CV4 7AL, UK.
E-mail: d.j.scanlan@warwick.ac.uk
[3]Current address: Unité d'Ecologie, Systématique et Evolution, Université Paris-Sud 11, 91405 Orsay cedex, France.
Received 19 October 2009; revised 18 February 2010; accepted 22 February 2010; published online 15 April 2010

(Marañón *et al.*, 2000; Poulton *et al.*, 2006; Morán, 2007). In conjunction with these carbon fixation measurements, the differentiated phytoplankton groups were phylogenetically affiliated using molecular techniques, including fluorescence *in situ* hybridization (FISH). In doing so, we reveal that small prymnesiophytes, mostly of taxonomic lineages lacking close cultured counterparts, can contribute significantly to CO_2 fixation in the ocean.

Materials and methods

Sampling and experimental design

Samples were collected on board the Royal Research Ship *Discovery* during cruise D326 in the subtropical and tropical northeast Atlantic Ocean between 12 January and 1 February 2008 at 18 stations encompassing an area between 12–26°N and 24–36°W (Figure 1). Seawater samples were collected at dawn with 10 or 20 l Niskin bottles mounted on a conductivity–temperature–fluorescence–depth profiler, with either trace-iron free titanium frame (10 l) or metallic frame (20 l). All samples were pre-filtered through 100 μm pore-size mesh when being decanted from the Niskin bottles, directly into 20 l hydrochloric acid washed polycarbonate carboys. Gas tight high-performance liquid chromatography glass vials (8 ml) were then filled with 7.8 ml of sampled water and inoculated with either 74 kBq $NaH^{14}CO_3$ for determining CO_2 fixation into total phototrophic biomass, or 7.4 MBq $NaH^{14}CO_3^-$ for assessing the contribution of the different groups of phototrophic microorganisms to CO_2 fixation. The vials were then incubated for up to 11 h—an average daylight period at the time of sampling. *In situ* light conditions on deck were monitored to be approximately 10% of direct sunlight, while the on deck incubation temperature varied <8.5%, on average, from *in situ* conditions. A set of samples was also incubated in the dark to ascertain dark CO_2 fixation. Up to 10 vial replicates incubated in the light and 5 vial replicates incubated in the dark were used for each experimental determination of total CO_2 fixation by phytoplankton. At each time point (~3 h), three of the replicate vials were used for CO_2 fixation measurement, two as duplicates for light conditions and one for dark conditions. Samples were fixed with 1% (w/v) final concentration paraformaldehyde (PFA—Sigma-Aldrich, Poole, UK) to preserve cell integrity (Zubkov and Leakey, 2009) to enable quantitative comparisons with flow cytometrically sorted cells (see below). Fixed cells were then harvested onto 0.2-μm pore-size polycarbonate filters and washed twice with deionized water. A filter was placed in a scintillation vial and 1 ml of 1% (v/v) HCl (Sigma-Aldrich) was added to securely purge the residue of inorganic carbon. Subsequently, 5 ml of scintillation cocktail was added to each vial. The vial content was mixed and left to equilibrate before radioassaying. Radioactivity retained in cells, harvested on filters, was measured using a liquid scintillation counter Tri-Carb 3100 (Perkin Elmer, Cambridge, UK) on board the ship.

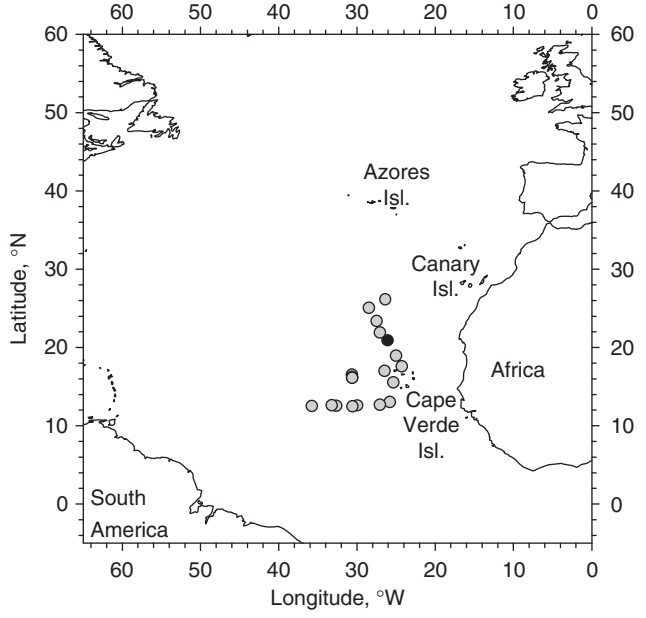

Figure 1 Schematic representation of the D326 cruise track. Circles indicate those stations at which CO_2 fixation experiments were performed. The black circle indicates the station (16400A) at which a sample used for clone library construction was collected.

Cell enumeration and flow cytometric sorting

Phytoplankton cells were enumerated by flow cytometry (FACSort—Becton Dickinson, NJ, USA) in seawater samples fixed with 1% (w/v) PFA final concentration to enable quantitative comparisons with flow cytometrically sorted cells. Previous work has shown no loss of either prokaryotic or eukaryotic cells occurs upon fixation (Zubkov and Burkill, 2006). *Synechococcus* cells were counted unstained (Zubkov *et al.*, 2000) while eukaryotic phytoplankton and *Prochlorococcus* were counted after staining with SYBR Green I (Sigma-Aldrich, 1:5000 dilution of the commercial stock; see Zubkov *et al.*, 2000, 2007). Multifluorescence 0.5-μm reference beads (fluoresbrite microparticles—Polysciences, Eppelheim, Germany) were used in all analyses as an internal standard for both fluorescence and flow rates. PFA-fixed, ^{14}C-labelled *Synechococcus* and *Prochlorococcus* cells were flow-sorted from unstained samples. PFA-fixed, ^{14}C-labelled eukaryotic cells were flow-sorted from SYBR Green I DNA-stained, unconcentrated samples. Flow sorting of both types of samples was completed within 10 h of fixation. The FACSort instrument was set at single-cell sort mode (the highest sorting purity of the instrument). Three to five proportional numbers (for example, 200, 400,

600, 800 and 1000 eukaryotes; 1000, 2000, 3000, 4000, 5000 and 6000 *Synechococcus*; 3000, 6000, 9000, 12 000, 15 000 and 18 000 *Prochlorococcus*) of cells for each target population were sorted. Sorted cells were collected onto 0.2-μm pore-size polycarbonate filters (Whatman, UK) and then processed as described above for the total samples. Mean cellular tracer incorporation by phytoplankton cells was determined by regression analysis ($r^2 > 0.97$, $P < 0.05$). To evaluate differences in CO_2 fixation rates among the different phytoplankton groups a two-tailed *t*-test was used ($P < 0.05$). To assess sorting recovery (Zubkov and Tarran, 2008) total ^{14}C fixation was determined in samples used for flow sorting by filtering six sub-samples (for example, 100, 150, 200, 300, 300 and 450 μl) onto 0.2-μm pore-size polycarbonate filters, washed twice with deionized water and radio-assayed as described above.

Fluorescent in situ hybridization

Seawater samples were amended with 0.05%. (v/v) pluronic solution (Sigma-Aldrich) final concentration to minimize clumping of concentrated cells. Samples (5 l) were then gently filtered through 0.2-μm pore-size CellTrap units (MEM-TEQ Ventures Ltd, Wigan, UK). Concentrated cells were washed off following the manufacturer's recommendations, fixed for 1 h at 4 °C with 1% (w/v) PFA, flash frozen in liquid nitrogen and then stored at −80 °C. Before sorting, samples were slowly defrosted on ice for 1 h and then stained with SYBR Green I (see above) for sorting eukaryotes or left unstained for sorting cyanobacteria. Samples were diluted with sterile seawater to obtain a flow cytometric counting rate of total particles <1000 particles per second. For each target group, 10 000–30 000-pigmented cells were sorted by flow cytometry based on endogenous phycoerythrin, chlorophyll *a* and stained DNA fluorescence signals (see above). Cells were then harvested onto 0.2-μm pore-size polycarbonate filters (Whatman), dehydrated in an ethanol series (50% (v/v), 80% (v/v) and 100% (v/v), 3 min each), dried at room temperature and stored at −80 °C until analysis. The 16S ribosomal RNA (rRNA) oligonucleotide probes used were PRO405 to target all known *Prochlorococcus* clades as well as the clade-specific probes 645LL, 645HLI and 645HLII (see West *et al*., 2001). For *Synechococcus*, the probes used targeted the following specific lineages: clade I (SYN1006), clade II (SYN1006RS), clade III (SYN262), clade IV (SYN635) or more generally clades I–VII and X (SYN1258). The nuclear 18S rRNA oligonucleotide probes used were EUK1209r, NCHLO01 and CHLO02 to target all eukaryotes and the class-specific probes PRAS01, PRAS02, PRAS05 (targeting prasinophytes), and CRYPTO13, PRYM02 and PELA01 targeting cryptophytes, prymnesiophytes and pelagophytes, respectively (Giovannoni *et al*., 1988; Simon *et al*., 1995, 2000; Biegala *et al*., 2003; Not *et al*., 2002, 2004). The chrysophyte-specific probe (CHRYSO1037) targeted the chloroplast 16S rRNA gene, as used previously for dot blot hybridization analysis (Fuller *et al*., 2006b) and validated here for tyramide signal amplification (TSA)-FISH analysis (see below). The protocol used for *in situ* hybridization with horseradish peroxidase-labelled probes has been previously described in Not *et al*. (2002) for the eukaryote-specific probes and in West *et al*. (2001) for the cyanobacterial-specific probes. In brief, before hybridization, cyanobacterial cells only were permeabilized by adding 30 μl lysozyme solution (5 mg ml^{-1} dissolved in 100 mM Tris-HCl, pH 8, 50 mM EDTA—Sigma-Aldrich) and incubated at 37 °C for 30 min. Filters were then rinsed with MilliQ water, dehydrated in an ethanol series (50% (v/v), 80% (v/v) and 100% (v/v), 3 min each) and then dried at room temperature. The formamide (Sigma-Aldrich) concentrations used in hybridization buffers containing horseradish peroxidase-labelled probes were as follows: CHRYSO1037, 20%; EUK1209r, NCHLO01, CHLO02, PRAS01, PRAS02, PRAS05, CRYPTO13, PRYM02, PELA01, 40%; 645LL, 645HLII, 50%; 645HLI, SYN1006, SYN1006RS, SYN262, SYN635, SYN1258, 55%. Oligonucleotide probes (2 μl of 50 ng μl^{-1} stock) were added to the hybridization buffer (variable % formamide, 0.9 M NaCl, 20 mM Tris-HCl, pH 7.5, 0.01% (w/v) sodium dodecyl sulphate [SDS]—Sigma-Aldrich) and incubated at 35 °C for 3–4 h. Filters were then washed twice for 20 min at 37 °C in washing buffer (56 mM NaCl, 5 mM EDTA, 0.01% (w/v) sodium dodecyl sulphate, 20 mM Tris-HCl, pH 7.5). Samples were equilibrated in TNT buffer (100 mM Tris-HCl, pH 7.5, 150 mM NaCl, 0.05% (v/v) Tween 20—Sigma-Aldrich) for 15 min at room temperature. TSA (individual fluorescein Tyramide reagent pack—Perkin Elmer) was performed for 30–40 min at room temperature in the dark in 10 μl of TSA mix following the manufacturer's recommendations. Filters were incubated twice at 55 °C for 20 min in TNT buffer and then dried at room temperature. Cells were counterstained with propidium iodide (final concentration 10 μg ml^{-1}) (Foulon *et al*., 2008) to visualize the nuclei. This allowed verification of labelling eukaryotic cells. Filters were then mounted in anti-fading reagent AF1 (Citifluor, London, UK). Cells were counted within 1 week (Not *et al*., 2002). The hybridized cells were counted under an Axioskop 40 (Zeiss, Jena, Germany) epifluorescence microscope equipped with a mercury light source and a Plan-Apochromat ×100 (Zeiss) objective. The green (fluorescein isothiocyanate) and red emission (propidium iodide) fluorescence produced by the different fluorochromes was collected between 510 and 550 nm and above 585 nm. Up to 350 positive cells were counted for the same sample and specific probe (data not shown). The average cell size of flow-sorted Euk-A and Euk-B cells was estimated using the fluorescein

isothiocyanate signal by measuring at least 500 cells from each group in different samples.

Chrysophyte probe validation and optimization for whole-cell hybridization

The chrysophyte probe used in this study was originally designed by Fuller *et al*. (2006b) for use in dot blot hybridization analysis and its specificity to chrysophytes has therefore been validated. However, probe specificity was re-checked using our in-house ARB database containing recently published and unpublished plastid 16S rRNA gene sequences as well as by BLASTn analysis. *In silico* testing without mismatches revealed that 94.1% of the eukaryotic sequences (64 of 68 retrieved) were affiliated with chrysophytes. When the four 'other' sequences were inserted into our ARB database, it became apparent that these environmental sequences also grouped with chrysophytes. This analysis also showed that the CHRYSO1037 probe encompassed both marine and freshwater Chrysophyceae, including groups without a cultured representative.

Conditions for *in situ* hybridization were optimized using different formamide concentrations in the hybridization buffer together with varying the NaCl concentration in the washing buffer. A marine chrysophyte enrichment culture obtained from the Porcupine Abyssal Plain Observatory in the North Atlantic (L Jardillier and DJ Scanlan, unpublished data) was used as a 'positive' control. Marine representatives of various other photosynthetic eukaryote classes were used as negative controls (Prasinophyceae: RCC827, RCC1124, RCC745; Trebouxiophyceae: RCC289; Chlorophyceae: RCC6; Cryptophyceae: RCC20; Bacillariophyceae: RCC70; Dinophyceae: RCC88; Pelagophyceae: RCC100; Bolidophyceae: RCC205; Prymnesiophyceae: RCC192). Bright and clear FISH signals were obtained with the 'positive' enrichment control while no hybridization was obtained in any of the negative control cultures using the optimized probe conditions. Moreover, a no-probe control showed there was no signal coming from potential endogenous horseradish peroxidases (data not shown).

DNA extraction, clone library construction and phylogenetic analysis

DNA was extracted from 30 000 flow-sorted Euk-B cells (station 16400A) concentrated on board following the same procedure as for the FISH method and filtered onto 13 mm diameter 0.2-μm. pore-size polycarbonate filters (Whatman). DNA was subsequently extracted using a protocol adapted from Fuller *et al*. (2003) and Neufeld *et al*. (2007). Briefly, cells were resuspended in 50 μl lysis buffer (0.75 M sucrose, 400 mM NaCl, 20 mM EDTA, 50 mM Tris-HCl [pH 9.0]—Sigma-Aldrich), and then 6 μl 10% (w/v) sodium dodecyl sulphate, 10 μl 10 mg ml^{-1} proteinase K (Roche, Welwyn Garden City, UK) added. The mix was incubated at 37 °C for 30 min, 55 °C for 10 min and then 2 μl 20 mg μl^{-1} glycogen (Roche) added to aid DNA recovery. After 5 min at room temperature, 150 μl 100% (v/v) ethanol was added and the DNA precipitated by centrifugation. The pellet was washed in 80% (v/v) ethanol and finally resuspended in 10 μl 10 mM Tris-HCl [pH 8.0], 0.1 mM EDTA. Plastid 16S rRNA gene sequences were amplified using primers PLA491F (Fuller *et al*., 2006a) and OXY1313R (West *et al*., 2001). PCR amplification was performed in a total reaction volume of 50 μl using 200 μM deoxynucleotide triphosphates, 1.2 mM $MgCl_2$, 0.4 μM of primers and 2.4 U *Taq* polymerase in 1 × enzyme buffer (Qiagen, Crawley, UK) with 1 mg ml^{-1} bovine serum albumin (Roche). Amplification conditions comprised 95 °C for 5 min followed by a step at 80 °C for 1 min when *Taq* polymerase was added. Then, 30 cycles were performed, of 95 °C for 30 s, 60 °C for 30 s and 72 °C for 40 s ended by a final extension at 72 °C for 6 min. PCR gene amplicons were cloned into pCR2.1-TOPO (Invitrogen, Paisley, UK). In all, 96 clones were chosen randomly and sequenced at the NERC Molecular Genetics Facility (Edinburgh, UK). Sequences were screened for the presence of chimeric artefacts using Chimera check from the Ribosomal Database Project II and Pintail software (http://www.bioinformatics-toolkit.org). Sequence alignment was performed using the ARB programme (Ludwig *et al*., 2004). The phylogenetic tree was constructed from sequences >1200 nucleotides in length using Jukes–Cantor correction and a maximum frequency filter for plastids that excluded alignment positions with sequence ambiguity or missing data. Shorter sequences were added by parsimony using the same filter. Bootstrap analysis was performed using the ARB parsimony bootstrap algorithm (Ludwig *et al*., 2004). The sequences reported in this paper have been deposited in Genbank under the following accession numbers: FJ797579–FJ797591 (see also Supplementary Table 1).

Results

Phytoplankton community composition

Photosynthetic eukaryotes ($2.2 \pm 1.2 \times 10^3$ cells ml^{-1}) were numerically the least abundant component of the phytoplankton, followed by *Synechococcus* ($1.5 \pm 1.6 \times 10^4$ cells ml^{-1}) and then *Prochlorococcus* (average cell number $2.1 \pm 0.8 \times 10^5$ cells ml^{-1}), (Figure 2a, Table 1). Within the eukaryotes, Euk-A were approximately twice as abundant ($1.4 \pm 1.1 \times 10^3$ cells ml^{-1}) as Euk-B ($0.6 \pm 0.2 \times 10^3$ cells ml^{-1}). Euk-B represented 0.18–0.43% of the total oxygenic phototrophic community and 0.04–0.10% of the total microbial community (Figure 2b).

On average Euk-A cells were 1.8 ± 0.1 μm in size and Euk-B cells 2.8 ± 0.2 μm (Table 1). The size of cyanobacteria (*Prochlorococcus* 0.5 ± 0.2 μm; *Synechococcus* 1.0 ± 0.3 μm) were determined by size

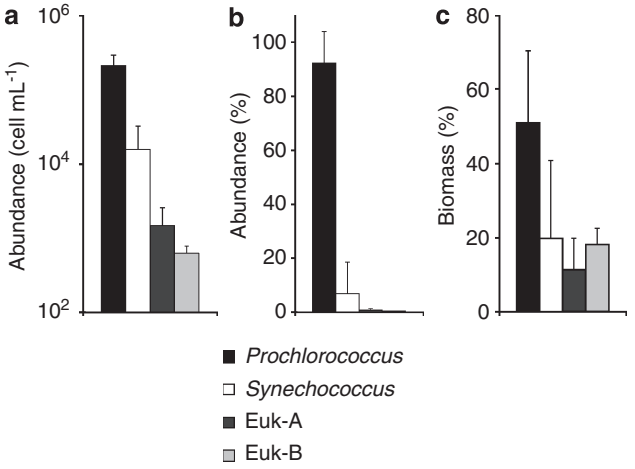

Figure 2 Composition of small phytoplankton in the studied area—(**a**) average cell abundance of the identified phytoplankton groups: *Prochlorococcus*, *Synechococcus*, and eukaryotes Euk-A and Euk-B; mean group % contribution to the total phytoplankton community in terms of (**b**) cell numbers and (**c**) biomass.

fractionation on earlier cruises in the same area (Zubkov *et al.*, 2000). A general biomass conversion factor of 0.22 pg C μm^{-3} was applied to biovolumes estimated from the cell sizes of the groups studied assuming a spherical shape (Table 1). Proportional to their numerical abundance, *Prochlorococcus* contributed the most to total phytoplankton biomass ($51 \pm 19\%$) followed by *Synechococcus* ($20 \pm 21\%$) (Figure 2c). The Euk-B group comprised $18 \pm 4\%$ of total phytoplankton biomass owing to their relatively large cell sizes in spite of their low cell number. Although twice more abundant than the Euk-B group, the Euk-A group contributed less ($11 \pm 8\%$) to phytoplankton biomass (Figure 2c).

Phytoplankton contribution to CO_2 fixation

Incorporation of ^{14}C tracer into total phototrophic biomass over the time of the incubation, as evidenced by regression analysis ($r^2 \geqslant 98\%$, $P < 0.05$), followed a simple sigmoidal curve, (Figure 3) indicating that phytoplankton cells were not physiologically impaired during the incubation process, for example, by the slight shifts in light and temperature conditions inherent to the experimental set up. There was no significant dark-driven CO_2 fixation, controls incubated in the dark being close to background (Figure 3). Nevertheless, the dark-fixation values were subtracted from light mediated CO_2 fixation rates. The average light CO_2 fixation rate across all 20 stations was 6.5 ± 3.0 mg C m^{-3} d^{-1}, with a maximum of 12.3 mg C m^{-3} d^{-1} observed close to the Cape Verde Islands (Table 2).

A second set of 100-times heavier ^{14}C-labelled samples was used to determine group-specific contribution to CO_2 fixation. The combined CO_2 fixation of the total photosynthetic eukaryotes, *Prochlorococcus* and *Synechococcus* fitted well the total CO_2 fixation measured ($101 \pm 7\%$) for the whole unsorted phytoplankton (Table 2). This indicated close to 100% recovery of flow-sorted cells (Zubkov and Tarran, 2008) as well as an absence of any other major CO_2-fixing groups in labelled samples, which remained unsorted. Hence, a CO_2 fixation budget for labelled samples could be ascertained. Owing to its high abundance, *Prochlorococcus* contributed $45 \pm 17\%$ to CO_2 fixation in spite of the low cell-specific rates (1.2 ± 0.6 fg C $cell^{-1}$ h^{-1}, Figures 4a and b, Table 2). Eukaryotes, on average, contributed approximately a third to total CO_2 fixation ($34 \pm 8\%$) measured on the whole unsorted phytoplankton largely because of high cell-specific rates (98 ± 50.0 fg C $cell^{-1}$ h^{-1}). Finally, *Synechococcus* contributed the least to primary production ($21 \pm 13\%$) because of moderate abundance and cell-specific CO_2 fixation rates (9.5 ± 4.3 fg C $cell^{-1}$ h^{-1}). Within the eukaryotes, the Euk-A group was responsible for between 7% and 19% of the total CO_2 fixed, because of the relatively low CO_2 fixation rates of this group (54.3 ± 19.0 fg C $cell^{-1}$ h^{-1}). In contrast, Euk-B had high CO_2 fixation rates (196 ± 72 fg C $cell^{-1}$ h^{-1}, Table 2) and in spite of their low abundance were responsible for 13–38% of the total CO_2 fixed. The biomass-specific CO_2 fixation rates (Figure 4c, Table 2) were not significantly different (*t*-test, $P < 0.05$) between the different functional groups analysed here (0.09 ± 0.04 mgC gC^{-1} h^{-1}) although the *Prochlorococcus* rate was lower (0.06 ± 0.03 mgC gC^{-1} h^{-1}).

Phytoplankton taxonomic composition

To ascertain the taxonomic composition of the different eukaryotic groups, that is, Euk-A and Euk-B, as well as *Prochlorococcus* and *Synechococcus* cyanobacteria, 10 000-pigmented cells from each group were sorted by flow cytometry from concentrated seawater samples at selected stations (see Materials and methods and Table 1) and identified by TSA-FISH (Schönhuber *et al.*, 1997) using class-specific oligonucleotides targeting the nuclear 18S rRNA, except for the chrysophytes were a chloroplast-targeted oligonucleotide probe was used (see Materials and methods). The groups observed by flow cytometry in concentrated samples (Supplementary Figure 1) were identical to those in non-concentrated samples used for the tracer work (see also Zubkov and Tarran, 2008) showing that cell integrity was unaltered by concentrating and processing of samples. For the eukaryotes, the Euk-B group was dominated by prymnesiophytes ($73 \pm 13\%$) (Figure 5a), with only minor contributions of pelagophytes ($2 \pm 2\%$) and chrysophytes ($8 \pm 8\%$) (Table 1). The Euk-A group comprised an assemblage of pelagophytes ($36 \pm 15\%$), chrysophytes ($26 \pm 15\%$) (Figure 5b) and prymnesiophytes ($16 \pm 11\%$).

Prasinophytes and cryptophytes, when detected, accounted for $<4\%$ of cells in either the Euk-A or

Table 1 Location, physical parameters, abundance and phytoplankton composition at the D326 stations sampled

Location	*Station*	*z (m)*	*Temp (°C)*	*Abundance ($\times 10^3$ cells ml^{-1})*					*Composition (%)*										*Size (μm)*	
				PRO	*SYN*	*EUK*	*Euk-A*	*Euk-B*	*PRO*	*SYN*			*Euk-A*			*Euk-B*			*Euk-A*	*Euk-B*
									HLII	*I*	*II*	*III*	*PRYM*	*PELA*	*CHRYS*	*PRYM*	*PELA*	*CHRYS*		
26°08.8′N, 26°24.9′W	16391A	5	22.2	287.5	2.3	0.9														
23°24.2′N, 27°31.0′W	16396 A	5	22.6	212.3	3.3	1.2			59	9	29	20	22	57	19	47	0	0	1.9	3.2
20°54.1′N, 26°07.2′W	16398 A	5	22.6	185.9	5.1	1.3														
18°57.2′N, 25°02.4′W	16400 A	5	22.1	56.3	26.7	2.1			68	10	71	4	3	32	33	69	0	13	1.6	2.9
17°35.3N, 24°18.3′W	16402 A	5	22.3	81.2	72.8	4.4				0	75	2	14	47	28	93	2	2	1.8	2.7
15°32.6′N, 25°23.4′W	16403 A	5	23.2	171.4	34.5	5.6	4.7	0.8												
13°01.1′N, 25°49.4′W	16405 B	5	24.5	373.3	9.0	1.7	1.1	0.7		0	36	20	4	31	26	79	3	13	2.1	2.7
12°38.8′N, 27°06.6W	16407 A	5	24.5	250.9	9.8	2.1														
12°35.4′N, 30°00.0′W	16409 A	5	24.3	326.2	28.5	4.3	2.5	0.8												
12°32.3′N, 32°41.2′W	16411 B	20	25.0	324.4	19.1	2.4	1.6	0.4	78	0	40	60	21	44	6	82	6	8	1.8	3.2
12°30.3′N, 35°46.7′W	16413 B	20	24.9	131.5	15.4	2.7	1.7	0.6												
12°35.4′N, 33°15.2′W	16415 B	20	24.6	182.4	23.9	2.4	1.6	0.5												
12°30.1′N, 30°36.6′W	16417 A	5	24.7	240.1	17.4	2.3	1.8	0.6												
16°07.3′N, 30°37.9′W	16418 A	5	23.5	243.7	8.4	1.6	0.7	0.8	74	0	0	76	4	14	55	73	0	4	1.7	2.8
16°07.8N, 30°38.1′W	16419 B	20	23.4	187.8	7.1	1.4	0.7	0.7												
16°12.2′N, 30°39.0′W	16422 B	20	23.5	213.0	4.9	1.1	0.5	0.7	77				35	19	31	74	1	25	1.9	2.8
16°13.1′N, 30°38.8′W	16425 B	20	22.5	212.4	4.7	1.1	0.4	0.7												
21°55.6′N, 27°05.0′W	16429 B	20	22.3	156.2	6.6	1.6	1.2	0.5												
25°04.4′N, 28°28.5′W	16431 B	20	21.9	220.5	6.0	1.8	1.2	0.4												
26°08.8′N, 26°24.9′W	16432 B	20	21.4	134.2	3.8	1.2	0.9	0.3	48	0	33	35	22	43	11	66	6	3	1.8	2.7
Mean			23.3	209.6	15.5	2.2	1.5	0.6	67	3	41	31	16	36	26	73	2	8	1.8	2.8
S.D.			1.1	80.0	16.5	1.3	1.1	0.2	12	4	26	28	11	15	15	13	2	8	0.1	0.2

Abbreviations: FISH, fluorescence *in situ* hybridization; TSA, tyramide signal amplification. Abundance of *Prochlorococcus* (PRO), *Synechococcus* (SYN), all eukaryotes (EUK), photosynthetic eukaryotes of group 'A' and 'B' (Euk-A and Euk-B, respectively) ($\times 10^3$ cells ml^{-1}). Percentage composition of *Prochlorococcus* ecotypes, *Synechococcus* clades and eukaryote classes was determined by TSA-FISH, cell size was measured by microscopy. Empty fields correspond to non-analysed samples.

Euk-B group. Phylogenetic analysis of 16S rRNA gene sequences obtained from a clone library constructed from flow-sorted Euk-B cells at one location (station 16400A) also showed a dominance of prymnesiophytes. Thus, of the 96 clones analysed, 64% were affiliated with prymnesiophytes including many sequences unrelated or poorly related (env SOL16400_NE12 and env SOL16400_NF03) to known cultured species (Figure 6). A more detailed phylogenetic characterization of the Euk-A and Euk-B groups will be presented elsewhere. As evidenced from the FISH data, there was remarkably little variation in taxonomic composition and size of the Euk-A and Euk-B groups (Table 1) indicating this community was largely homogeneous over the course of the study. Averaged over all stations *Prochlorococcus* comprised mainly (67 ± 12%) cells belonging to the HLII lineage while *Synechococcus* was composed largely of members of clade II (41 ± 26%) and clade III (31 ± 28%) (Table 1) (see Fuller *et al*., 2003 for clade designations).

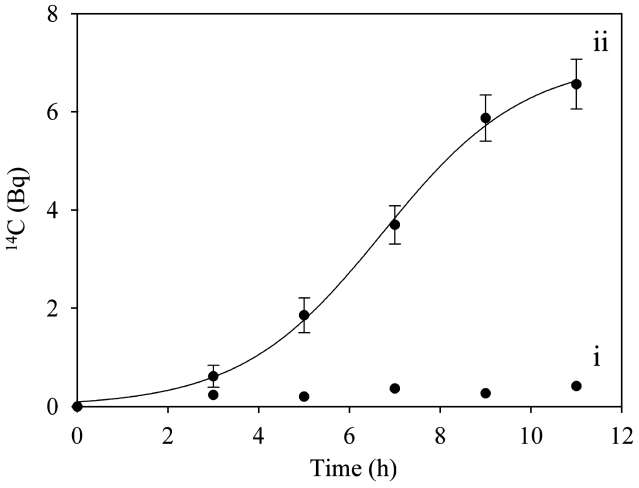

Figure 3 Sigmoid regression approximation ($r^2 \geqslant 98\%$, $P < 0.05$) of total phytoplankton ^{14}C uptake (Bq) (i) in the dark and (ii) in *in situ* simulated light conditions during the time course (h) of a typical tracer experiment.

Discussion

Assessment of phytoplankton group-specific CO_2 fixation by direct radiotracer incorporation has made little progress since the seminal study of Li (1994). In slight contrast to the Li study, however, here we used flow cytometric sorting of fixed cells to determine the precise contribution of different functional groups to CO_2 fixation into biomass, because we believe this provides more reproducible estimates compared with sorting of live cells (see Larsen *et al*., 2008). We should point out though, that while measurement of phytoplankton CO_2 fixation using a ^{14}C radiotracer has been used for decades (Steemann-Nielsen, 1952) offering high precision (Irwin, 1991), the method does have some

Table 2 CO_2 fixation rates at stations along the D326 cruise track in the tropical North Atlantic

	CO_2 fixation rates ([a]mgC m^{-3} d^{-1}; [b]fgC Cell^{-1} h^{-1}; [c]mgC gC^{-1} h^{-1})										*Contribution to CO_2 fixation (%)*				
	Total[a]	*PRO*[b]	*SYN*[b]	*EUK*[b]	*Euk-A*[b]	*Euk-B*[b]	*PRO*[c]	*SYN*[c]	*Euk-A*[c]	*Euk-B*[c]	*PRO*	*SYN*	*EUK*	*Euk-A*	*Euk-B*
16391 A	2.5	0.6	3.4	32.0			0.03	0.03			83	4	14		
16396 A	3.3	0.7	5.8	100.3			0.04	0.06			53	7	41		
16398 A	4.2	1.4	7.7	56.7			0.07	0.08			70	11	19		
16400 A	5.1	2.4	6.1	71.6			0.12	0.06			30	37	34		
16402 A	10.5	2.3	5.9	69.3			0.12	0.06			20	47	33		
16403 A	9.7	1.3	9.6	59.9	38.5	260.3	0.07	0.10	0.06	0.11	26	40	40	19	21
16405 B	6.4	1.0	4.2	86.6	37.1	155.3	0.05	0.04	0.06	0.07	67	7	26	7	19
16407 A	6.1	0.9	8.0	90.7			0.05	0.08			45	15	37		
16409 A	12.3	1.2	13.5	71.2	55.1	238.9	0.06	0.14	0.09	0.10	36	36	29	12	17
16411 B	8.7	0.9	11.3	91.9	67.7	209.0	0.05	0.11	0.11	0.09	38	29	30	16	13
16413 B	8.6	2.1	14.8	116.2	85.5	365.5	0.11	0.15	0.14	0.16	37	30	41	16	25
16415 B	8.9	0.8	9.4	117.1	58.1	185.9	0.04	0.09	0.10	0.08	20	29	37	18	19
16417 A	9.6	1.3	15.7	115.8		239.0	0.07	0.16		0.10	39	33	32		32
16418 A	4.4	0.9	5.0	89.6	41.5	174.5	0.05	0.05	0.07	0.08	56	11	38	7	31
16419 A	9.4	1.9	17.1	258.4	89.4	425.5	0.10	0.17	0.15	0.19	44	15	44	7	37
16422 B	4.2	1.1	7.7	134.4	39.3	285.9	0.06	0.08	0.06	0.12	63	10	42	4	38
16425 B	5.2	1.1	8.7	150.7		165.0	0.06	0.09		0.07	53	9	37		37
16429 B	6.0	0.8	15.1	139.7	48.8	248.2	0.04	0.15	0.08	0.11	25	19	44	14	30
16431 B	1.8	0.3	6.3	33.6	30.1	105.6	0.02	0.06	0.05	0.05	47	24	39	17	22
16432 B	3.6	1.4	14.5	73.3	60.1	162.8	0.07	0.15	0.10	0.07	58	18	29	14	14
Mean	6.5	1.2	9.5	98.0	54.3	230.1	0.06	0.09	0.09	0.10	45	21	34	13	25
S.D.	3.0	0.6	4.3	50.0	19.0	86.1	0.03	0.04	0.03	0.04	17	13	8	5	9

Rates are presented for the total phytoplankton population (mg C m^{-3} d^{-1}), *Prochlorococcus* (PRO), *Synechococcus* (SYN), all eukaryotes (EUK) as well as photosynthetic eukaryotes of groups 'A' and 'B' (Euk-A and Euk-B, respectively). The percentage contribution of *Prochlorococcus*, *Synechococcus*, Euk-A or Euk-B to the total CO_2 fixed is also presented. Empty fields correspond to non-analysed samples.

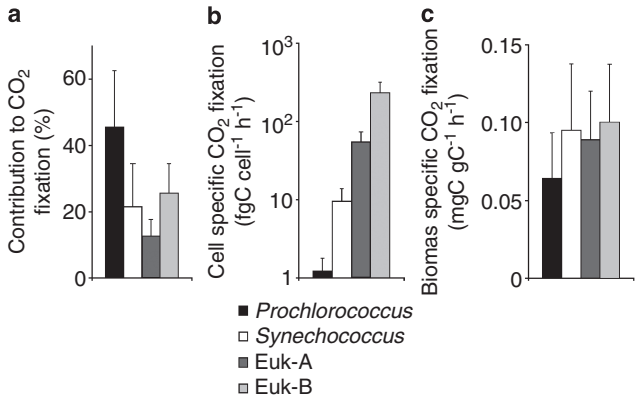

Figure 4 (**a**) Contribution of the phytoplankton groups *Prochlorococcus*, *Synechococcus*, and eukaryotes Euk-A and Euk-B, to total phytoplankton CO_2 fixation (**b**) cell-specific CO_2 fixation rates (fgC cell^{-1} h^{-1}) averaged over all stations sampled and (**c**) biomass-specific CO_2 fixation rates (mgC gC^{-1} h^{-1}) averaged at stations sampled wherein data were available for all phytoplankton functional groups.

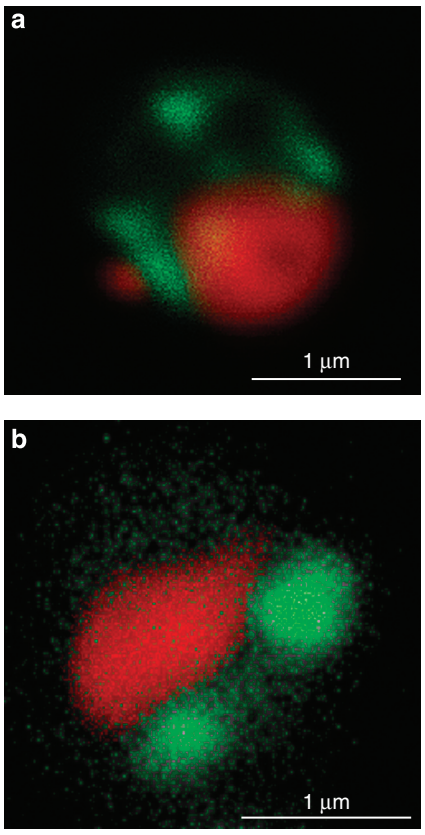

Figure 5 Fluorescence microscope image of a typical cell that was positively labelled with (**a**) the prymnesiophyte-specific probe or (**b**) the chrysophyte-specific probe. Green colour shows the positive signal of the horseradish peroxidase (HRP)-labelled probes (**a**) in the plastids and (**b**) in the whole cell while the red colour corresponds to the nucleus stained with propidium iodide.

drawbacks including the low specific activity of labelling because of the high natural concentration of (bi)carbonate in seawater. Indeed, ^{14}C added as dissolved inorganic carbon gradually enters pools of particulate and dissolved organic matter. Therefore, in long incubations the dynamics of the labelled carbon cannot accurately represent all transformations between organic and inorganic carbon pools (for example, respiration). Nonetheless, control sortings of heterotrophic bacterioplankton showed no measurable uptake of tracer into biomass (unpublished data) and hence, we feel justified that the ^{14}C radiotracer method can accurately trace inorganic C assimilation into individual phytoplankton cells. However, as potential light respiration of fixed carbon by phytoplankton cells could occur, the reported specific rates of CO_2 fixation into cell biomass should be treated as lower or net estimates.

The total CO_2 fixation rates reported here (Figure 4, Table 2) are comparable to previous measurements (for example, see Landry *et al.*, 2000; Pérez *et al.*, 2006; Morán, 2007). Moreover, the large contribution of small phytoplankton (that is, *Prochlorococcus*, *Synechococcus*, Euk-A and Euk-B) to CO_2 fixation reported here (Figure 4) is also in agreement with previous size-fractionation studies (for example, see Marañón *et al.*, 2001; Pérez *et al.*, 2006). Indeed, Goericke (1998) observed that the contribution to chlorophyll *a* and primary production of phytoplankton $<3\,\mu m$ in size was almost constant over the year at a station southeast of Bermuda representing as much as 79% of the total.

Despite Euk-B being the Euk-B being the least abundant phytoplankton group, its contribution to oceanic CO_2 fixation reached 38% of total primary production (Table 2). Given the average cell size of the different functional groups, we might have expected that smaller cells would have competed more efficiently for resources (Raven, 1998) because of their high surface area to volume ratios. However, the opposite result confirms that CO_2 uptake is more dependent on biovolume than nutrient uptake rates. Interestingly, the lower biomass-specific CO_2 fixation rates of *Prochlorococcus* (Figure 4c) compared with the other functional groups analysed might be explained if *Prochlorococcus* cells can use harvested light not only for CO_2 fixation but also for directly producing adenosine triphosphate to fuel nutrient uptake including the acquisition of organic molecules (Zubkov, 2009). Certainly, it is clear that the Euk-B cells are important carbon fixers because of their high contribution to CO_2 fixation in spite of their low cell number. In addition, it is possible that, in spite of their small size, they can participate directly or indirectly to carbon export from the surface ocean (Richardson and Jackson, 2007). This facet may be more pronounced given that small phytoplankton $<5\,\mu m$ in size can also obtain significant carbon intake through bacterivory (Zubkov and Tarran, 2008).

While members of the Prasinophyceae, especially *Micromonas* spp., are now widely recognized as being the dominant component of the eukaryotic

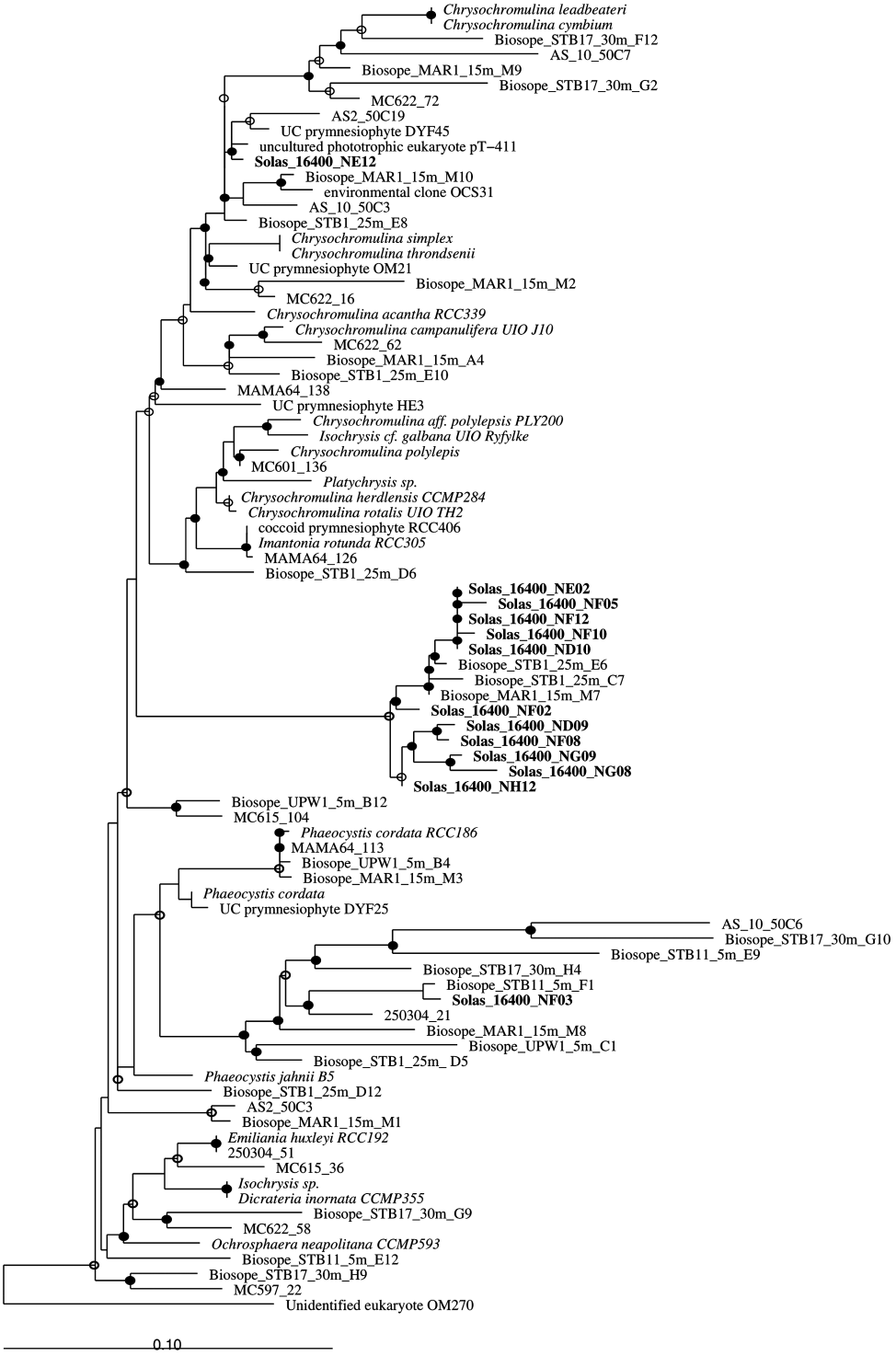

Figure 6 Neighbour joining tree of 16S rRNA gene sequences from marine algal plastids including new sequences derived from flow-sorted Euk-B cells at station 16400A. Bootstrap analysis was performed with ARB parsimony bootstrap (Ludwig *et al.*, 2004). ●: values > 90%; ○: 70–90%; values <70% are not shown. Environmental sequences are as follows: Solas: clones from the D326 cruise; AS: clones from the Arabian Sea (Fuller *et al.*, 2006a); MC and MAMA: clones from the Gulf of Naples (McDonald *et al.*, 2007); DYF: clones from the northwest Mediterranean Sea Dyfamed station (Marie *et al.*, 2006); Biosope: clones from the southeast Pacific Ocean (Lepère *et al.*, 2009).

picophytoplankton in coastal environments (Not *et al.*, 2004; Vaulot *et al.*, 2008), much less is known of the composition of these communities in open ocean waters. The low proportion of prasinophytes observed in this study (Table 1) is consistent then with *Micromonas* spp. cell numbers decreasing

rapidly in open ocean waters (Not *et al.*, 2008). However, our use of the PRAS02 probe that targets all Mamiellales except *Bathycoccus* spp. could lead to the slight underestimation of prasinophytes here, and especially of this latter genus.

While pelagophytes appear to be widely distributed in these environments, though generally found at lower abundance than in this study (Bidigare and Ondrusek, 1996; Díez *et al.*, 2001; Moon–van der Staay *et al.*, 2001; Wilmotte *et al.*, 2002; Romari and Vaulot, 2004; Fuller *et al.*, 2006b; McDonald *et al.*, 2007), there are few reports of members of the class Chrysophyceae in marine systems. While some 'photosynthetic' chrysophytes have been observed by microscopy, these are not abundant and usually refer to cells larger than 5 μm (Throndsen, 1996; Novarino *et al.*, 1997). The exception is the order Parmales that encompass a group of small (<5 μm in diameter), siliceous cells, each with a chloroplast (Booth and Marchant, 1987; Bravo–Sierra and Hernández–Becerril, 2003). However, the chrysophytes observed by microscopy and TSA-FISH here had two chloroplasts, no apparent siliceous deposits in the outer membrane (that is, their 90° light scatter was similar to other eukaryotic cells) and were smaller than 2.5 μm (Figure 5b). Moreover, plastid 16S rRNA gene sequences of photosynthetic chrysophytes have recently been reported from various marine environments (Fuller *et al.*, 2006a, b; McDonald *et al.*, 2007; Lepère *et al.*, 2009) highlighting the potentially wide distribution and ecological importance of this class. Furthermore, 18S rRNA gene sequences of marine chrysophytes forming new groups without cultured representatives and comprising putative photosynthetic organisms have also been retrieved in several recent studies (Worden and Not, 2008; Shi *et al.*, 2009).

Prymnesiophytes were clearly the main component of the Euk-B fraction as determined by FISH analysis. Plastid 16S rRNA gene sequences obtained through clone library construction of sorted Euk-B cells allowed us to ascertain more accurately the composition of the Euk-B group. Subsequent phylogenetic analysis (Figure 6) showed that these prymnesiophytes were closely related to environmental sequences retrieved from the southeast Pacific Ocean encompassing some of the most oligotrophic waters on earth (Lepère *et al.*, 2009) suggesting these lineages have a wide geographic distribution. Moreover, the majority of these sequences were taxonomically affiliated with lineages with no close cultured counterpart. While prymnesiophytes appear widespread in most mesotrophic and oligotophic waters (Bidigare and Ondrusek, 1996; Moon-van der Staay *et al.*, 2000; Díez *et al.*, 2001; Wilmotte *et al.*, 2002; Fuller *et al.*, 2006b; Lepère *et al.*, 2009) and can contribute from 30% to 50% of total photosynthetic standing stock across the world ocean (Liu *et al.*, 2009), cultured representatives of the size fractions reported here are still rare. The prymnesiophytes observed in this study are likely not calcified as shown both by microscopy (Figure 5a) and their flow cytometry signature (that is, their 90° light scatter was similar to other eukaryotic cells) (Supplementary Figure 1) reinforcing the assertion that these prymnesiophytes include novel groups. Indeed, Young *et al.* (2005) have suggested coccolithophorids represent less than half the existing diversity of Haptophyta. Other studies are beginning to describe the extensive diversity within Haptophyta <3 μm in size (Worden and Not, 2008; Liu *et al.*, 2009). Moreover, recent work (Urein *et al.*, 2007; Zubkov and Tarran, 2008) suggests that oceanic mixotrophy by plastid-containing protists is dominated by small Haptophyta-like cells, consistent with both photoautotrophic and mixotrophic trophic modes being observed in cultured prymnesiophytes (for example, *Chrysochromunlina* sp. and *Prymnesium parvum* see Kawachi *et al.*, 1991; Jones *et al.*, 1995).

The key role of prymnesiophytes in marine CO_2 fixation we show here, is entirely consistent with new estimates of depth-integrated relative abundance of 19′-hexanoyloxyfucoxanthin, an accessory pigment considered characteristic of Haptophyta (though also present in a few other Heterokont algae, see Andersen, 2004), which indicate haptophytes dominate chlorophyll-*a*-normalized phytoplankton standing stock in the modern ocean (Liu *et al.*, 2009). Further group-specific CO_2 fixation data collected at basin scales will be critical to assess the significance of these prymnesiophytes in global primary production. These data will also help to validate models that estimate ocean productivity using chlorophyll *a*-based fluorescence measurements (Behrenfeld *et al.*, 2001). The next crucial step, beyond identification and assessment of their metabolic activities, will be to address the autoecology of the dominant photosynthetic eukaryotes by dissecting the biotic and abiotic factors that control their proliferation in the Ocean (Amann and Fuchs, 2008). Thus, the revealed major role for the prymnesiophyte-dominated phytoplankton group in photosynthetic CO_2 fixation in the subtropical and tropical northeast Atlantic Ocean should be considered an important stepping stone towards understanding the Oceans' productivity.

Acknowledgements

We gratefully acknowledge the captain, officers and crew aboard the RRS *Discovery* for their help during the cruise. We thank Eric Achterberg and other scientists, involved in the Natural Environment Research Council (NERC) UK Surface Ocean Lower Atmosphere Study (SOLAS) project NE/C001931/1, for an opportunity given to LJ to participate in the cruise. We also thank I Mary for advice on the cell concentrating procedure, W Gaze for sharing microscope facilities, F LeGall and D Vaulot for sharing cultures of the Roscoff Culture Collection and L Lehtovirta and M Nicoll for optimizing the DNA extraction protocol

from sorted cells. This study was supported by NERC grant NE/C003160/1 and a NERC funded PhD studentship to JP.

Authors contribution: DJS and MZ designed the study. Tracer work, FISH counts and data analysis was carried out by LJ. Flow cytometry work was performed by MVZ on board and by LJ ashore. JP and LJ constructed the genetic libraries. LJ, MVZ and DJS wrote the paper.

References

Amann R, Fuchs BM. (2008). Single–cell identification in microbial communities by improved fluorescence *in situ* hybridization techniques. *Nature Rev* **6**: 339–348.

Andersen RA. (2004). Biology and systematics of heterokont and haptophyte algae. *Am J Bot* **91**: 1508–1522.

Behrenfeld MJ, Randerson JT, McClain CR, Feldman GC, Los SO, Tucker CJ *et al.* (2001). Biospheric primary production during an ENSO transition. *Science* **291**: 2594–2597.

Bidigare RR, Ondrusek ME. (1996). Spatial and temporal variability of phytoplankton pigment distributions in the central equatorial Pacific Ocean. *Deep–Sea Res II* **43**: 809–833.

Biegala IC, Not F, Vaulot D, Simon N. (2003). Quantitative assessment of picoeukaryotes in the natural environment by using taxon-specific oligonucleotide probes in association with tyramide signal amplification-fluorescence *in situ* hybridization and flow cytometry. *Appl Environ Microbiol* **69**: 5519–5529.

Booth BC, Marchant HJ. (1987). Parmales, a new order of marine chrysophytes, with descriptions of three new genera and seven new species. *J Phycol* **23**: 245–260.

Bravo–Sierra E, Hernández–Becerril DU. (2003). Parmales (Chrysophyceae) from the Gulf of Tehuantepec, Mexico, including the description of a new species, *Tetraparma insecta* sp nov, and a proposal to the taxonomy of the group. *J Phycol* **39**: 577–583.

Díez B, Pedrós–Alío C, Massana R. (2001). Study of genetic diversity of eukaryotic picoplankton in different oceanic regions by small–subunit rRNA gene cloning and sequencing. *Appl Environ Microbiol* **67**: 2932–2941.

Foulon E, Not F, Jalabert F, Cariou T, Massana R, Simon N. (2008). Ecological niche partitioning in the picoplanktonic green alga *Micromonas pusilla*: evidence from environmental surveys using phylogenetic probes. *Environ Microbiol* **10**: 2433–2443.

Fuller NJ, Campbell C, Allen DJ, Pitt FD, Zwirglmaier K, Le Gall F *et al.* (2006a). Analysis of photosynthetic picoeukaryote diversity at open ocean sites in the Arabian Sea using a PCR biased towards marine algal plastids. *Aquat Microb Ecol* **43**: 79–93.

Fuller NJ, Marie D, Partensky F, Vaulot D, Post AF, Scanlan DJ. (2003). Clade–specific 16S ribosomal DNA oligonucleotides reveal the predominance of a single marine *Synechococcus* clade throughout a stratified water column in the Red Sea. *Appl Environ Microbiol* **69**: 2430–2443.

Fuller NJ, Tarran GA, Cummings DG, Woodward EMS, Orcutt KM, Yallop M *et al.* (2006b). Molecular analysis of photosynthetic picoeukaryote community structure along an Arabian Sea transect. *Limnol Oceanogr* **51**: 2502–2514.

Giovannoni SJ, Delong EF, Olsen GJ, Pace NR. (1988). Phylogenetic group–specific oligonucleotide probes for identification of single microbial cells. *J Bacteriol* **170**: 720–726.

Goericke R. (1998). Response of phytoplankton community structure and taxon-specific growth rates to seasonally varying physical forcing in the Sargasso Sea off Bermuda. *Limnol Oceanogr* **43**: 921–935.

Grob C, Ulloa O, Claustre H, Huot Y, Alarcón G, Marie D. (2007). Contribution of picoplankton to the total particulate organic carbon (POC) concentration in the eastern South Pacific. *Biogeosci Discuss* **4**: 1–37.

Irwin B. (1991). Coulometric measurement of primary production, with comparison against dissolved oxygen and ^{14}C methods in a seasonal study. *Mar Ecol Prog Ser* **71**: 97–102.

Jones HLJ, Durjun P, Leadbeater BSC, Green JC. (1995). The relationship between photoacclimation and phagotrophy with respect to chlorophyll *a*, carbon and nitrogen content, and cell size of *Chrysochromulina brevifilum* (Prymnesiophyceae). *Phycologia* **34**: 128–134.

Kawachi M, Inouye I, Maeda O, Chihara M. (1991). The haptonema as a food-capturing device: observations on *Chrysochromulina hirta* (Prymnesiophyceae). *Phycologia* **30**: 563–573.

Landry MR, Constantinou J, Latasa M, Brown SL, Bidigare RR, Ondrusek ME. (2000). Biological response to iron fertilization in the eastern equatorial Pacific (IronEx II). III. Dynamics of phytoplankton growth and microzooplankton grazing. *Mar Ecol Prog Ser* **201**: 57–72.

Larsen A, Tanaka T, Zubkov MV, Thingstad TF. (2008). P-affinity measurements of specific osmotroph populations using cell-sorting flow cytomtery. *Limnol Oceanogr Meth* **6**: 355–363.

Latasa M, Bidigare RR. (1998). A comparison of phytoplankton populations of the Arabian Sea during the spring intermonsoon and southwest monsoon of 1995 as described by HPLC-analyzed pigments. *Deep Sea Res Pt II* **45**: 2133–2170.

Lepère C, Vaulot D, Scanlan DJ. (2009). Photosynthetic picoeukaryote community structure in the south east Pacific Ocean encompassing the most oligotrophic waters on Earth. *Environ Microbiol* **11**: 3105–3117.

Li WKW. (1994). Primary productivity of prochlorophytes, cyanobacteria, and eucaryotic ultraphytoplankton: measurements from flow cytometric sorting. *Limnol Oceanogr* **39**: 169–175.

Liu H, Aris-Brosou S, Probert I, de Vargas C. (2010). A timeline of the environmental genetics of the haptophytes. *Mol Biol Evol* **27**: 161–176.

Liu H, Probert I, Uitz J, Claustre H, Aris-Brosou S, Frada M *et al.* (2009). Extreme diversity in noncalcifying haptophytes explains a major pigment paradox in open oceans. *Proc Natl Acad Sci USA* **106**: 12803–12808.

Ludwig W, Strunk O, Westram R, Richter L, Meier H, Yadhukumar *et al.* (2004). ARB: a software environment for sequence data. *Nucl Acids Res* **32**: 1363–1371.

Marañón E, Holligan PM, Barciela R, Gonzalez N, Mourino B, Pazo MJ *et al.* (2001). Patterns of phytoplankton size structure and productivity in contrasting open-ocean environments. *Mar Ecol Prog Ser* **216**: 43–56.

Marañón E, Holligan PM, Varela M, Mouriño B, Bale AJ. (2000). Basin–scale variability of phytoplankton biomass, production and growth in the Atlantic Ocean. *Deep–Sea Res I* **47**: 825–857.

Marie D, Zhu F, Balagúe V, Ras J, Vaulot D. (2006). Eukaryotic picoplankton communities of the Mediterranean Sea in summer assessed by molecular approaches (DGGE, TTGE, QPCR). *FEMS Microbiol Ecol* **55**: 403–415.

McDonald SM, Sarno D, Scanlan DJ, Zingone A. (2007). Genetic diversity of eukaryotic ultraphytoplankton in the Gulf of Naples during an annual cycle. *Aquat Microb Ecol* **50**: 75–89.

Moon–van der Staay SY, De Wachter R, Vaulot D. (2001). Oceanic 18S rDNA sequences from picoplankton reveal unsuspected eukaryotic diversity. *Nature* **409**: 607–610.

Moon-van der Staay SY, van der Staay GWM, Guillou L, Vaulot D. (2000). Abundance and diversity of prymnesiophytes in the picoplankton community from the equatorial Pacific Ocean inferred from 18S rDNA sequences. *Limnol Oceanogr* **45**: 98–109.

Morán XAG. (2007). Annual cycle of picophytoplankton photosynthesis and growth rates in a temperate coastal ecosystem: a major contribution to carbon fluxes. *Aquat Microb Ecol* **49**: 267–279.

Neufeld JD, Vohra J, Dumont MG, Lueders T, Manefield M, Friedrich MW *et al.* (2007). DNA stable–isotope probing. *Nat Methods* **2**: 860–866.

Not F, Latasa M, Marie D, Cariou T, Vaulot D, Simon N. (2004). A single species *Micromonas pusilla* (Prasinophyceae) dominates the eukaryotic picoplankton in the western English Channel. *Appl Environ Microbiol* **70**: 4064–4072.

Not F, Latasa M, Scharek R, Viprey M, Karleskind P, Balague V *et al.* (2008). Protistan assemblages across the Indian Ocean, with a specific emphasis on the picoeukaryotes. *Deep-Sea Res I* **55**: 1456–1473.

Not F, Simon N, Biegala IC, Vaulot D. (2002). Application of fluorescent *in situ* hybridization coupled with tyramide signal amplification (FISH-TSA) to assess eukaryotic picoplankton composition. *Aquat Microb Ecol* **28**: 157–166.

Novarino G, Mills DK, Hannah F. (1997). Pelagic flagellate populations in the southern North Sea, 1988–89. I. Qualitative observations. *J Plankton Res* **19**: 1081–1109.

Pérez V, Fernández E, Marañón E, Morán XAG, Zubkov MV. (2006). Vertical distribution of phytoplankton biomass, production and growth in the Atlantic subtropical gyres. *Deep–Sea Res I* **53**: 1616–1634.

Poulton AJ, Holligan PM, Hickman A, Kim YN, Adey TR, Stinchcombe MC *et al.* (2006). Phytoplankton carbon fixation, chlorophyll–biomass and diagnostic pigments in the Atlantic Ocean. *Deep–Sea Res II* **53**: 1593–1610.

Raven JA. (1998). The twelfth tansley lecture. Small is beautiful: the picophytoplankton. *Functional Ecol* **12**: 503–513.

Richardson TL, Jackson GA. (2007). Small phytoplankton and carbon export from the surface ocean. *Science* **315**: 838–840.

Romari K, Vaulot D. (2004). Composition and temporal variability of picoeukaryote communities at a coastal site of the English Channel from 18S rDNA sequences. *Limnol Oceanogr* **49**: 784–798.

Schönhuber W, Fuchs B, Juretschko S, Amann R. (1997). Improved sensitivity of whole–cell hybridization by the combination of horseradish peroxidase–labeled oligonucleotides and tyramide signal amplification. *Appl Environ Microbiol* **63**: 3268–3273.

Shi XL, Marie D, Jardillier L, Scanlan DJ, Vaulot D. (2009). Groups without cultured representatives dominate eukaryotic picophytoplankton in the oligotrophic south east Pacific Ocean. *PLoS One* **4**: e7657.

Simon N, Campbell L, Ornolfsdottir E, Groben R, Guillou L, Lange M *et al.* (2000). Oligonucleotide probes for the identification of three algal groups by dot blot and fluorescent whole–cell hybridization. *J Euk Microbiol* **47**: 76–84.

Simon N, Lebot N, Marie D, Partensky F, Vaulot D. (1995). Fluorescent *in situ* hybridization with rRNA–targeted oligonucleotide probes to identify small phytoplankton by flow cytometry. *Appl Environ Microbiol* **61**: 2506–2513.

Steemann-Nielsen E. (1952). The use of radioactive carbon (^{14}C) for measuring organic production in the sea. *J Cons Int Explor Mer* **18**: 117–140.

Teira E, Mourino B, Marañón E, Perez V, Pazo MJ, Serret P *et al.* (2005). Variability of chlorophyll and primary production in the Eastern North Atlantic Subtropical Gyre: potential factors affecting phytoplankton activity. *Deep–Sea Res I* **52**: 569–588.

Throndsen J. (1996). The planktonic marine flagellates. In: Tomas CR (ed). *Identifying Marine Phytoplankton*. Academic Press: San Diego, pp 591–730.

Urein F, Massana R, Alonso-Sáez L, Gasol JM. (2007). Significant year-round effect of small mixotrophic flagellates on bacterioplankton in an oligotrophic coastal system. *Limnol Oceanogr* **52**: 456–469.

Vaulot D, Eikrem W, Viprey M, Moreau H. (2008). The diversity of small eukaryotic phytoplankton ($<3\,\mu m$) in marine ecosystems. *FEMS Microbiol Rev* **32**: 795–820.

Viprey M, Guillou L, Ferréol M, Vaulot D. (2008). Wide genetic diversity of picoplanktonic green algae (Chloroplastidia) in the Mediterranean Sea uncovered by a phylum-biased PCR approach. *Environ Microbiol* **10**: 1804–1822.

West NJ, Schönhuber WA, Fuller NJ, Amann RI, Rippka R, Post AF *et al.* (2001). Closely related *Prochlorococcus* genotypes show remarkably different depth distributions in two oceanic regions as revealed by *in situ* hybridisation using 16S rRNA–targeted oligonucleotides. *Microbiology* **147**: 1731–1744.

Wilmotte A, Demonceau C, Goffart A, Hecq JH, Demoulin V, Crossley AC. (2002). Molecular and pigment studies of the picophytoplankton in a region of the Southern Ocean (42–541S, 141–1441E) in March 1998. *Deep–Sea Res II* **49**: 3351–3363.

Worden AZ, Nolan JK, Palenik B. (2004). Assessing the dynamics and ecology of marine picophytoplankton: the importance of the eukaryotic component. *Limnol Oceanogr* **49**: 168–179.

Worden AZ, Not F. (2008). Ecology and diversity of picoeukaryotes. In: Kirchman DL (ed). *Microbial Ecology of the Ocean*. John Wiley & Sons, Inc.: New York, pp 159–196.

Wright SW, Ishikawa A, Marchant HJ, Davidson AT, van den Enden RL, Nash GV. (2009). Composition and significance of picophytoplankton in Antarctic waters. *Polar Biol* **32**: 797–808.

Young JR, Geisen M, Probert I. (2005). A review of selected aspects of coccolithophore biology with implications for paleobiodiversity estimation. *Micropaleontology* **51**: 267–288.

Zubkov MV. (2009). Photoheterotrophy in marine prokaryotes. *J Plankton Res* **31**: 933–938.

Zubkov MV, Sleigh MA, Burkill PH, Leakey RJG. (2000). Picoplankton community structure on the Atlantic Meridional Transect: a comparison between seasons. *Prog Oceanogr* **45**: 369–386.

Zubkov MV, Burkill PH. (2006). Syringe pumped high speed flow cytometry of oceanic phytoplankton. *Cytometry Part A* **69A**: 1010–1019.

Zubkov MV, Burkill PH, Topping JN. (2007). Flow cytometric enumeration of DNA stained oceanic planktonic protists. *J Plankton Res* **29**: 79–86.

Zubkov MV, Leakey RJ. (2009). Evaluation of the efficiency of metabolism of dinoflagellate phosphorus and carbon by a planktonic ciliate. *Eur J Protist* **45**: 166–173.

Zubkov MV, Tarran GA. (2008). High bacterivory by the smallest phytoplankton in the North Atlantic Ocean. *Nature* **455**: 224–227.

Supplementary Information accompanies the paper on The ISME Journal website (http://www.nature.com/ismej)

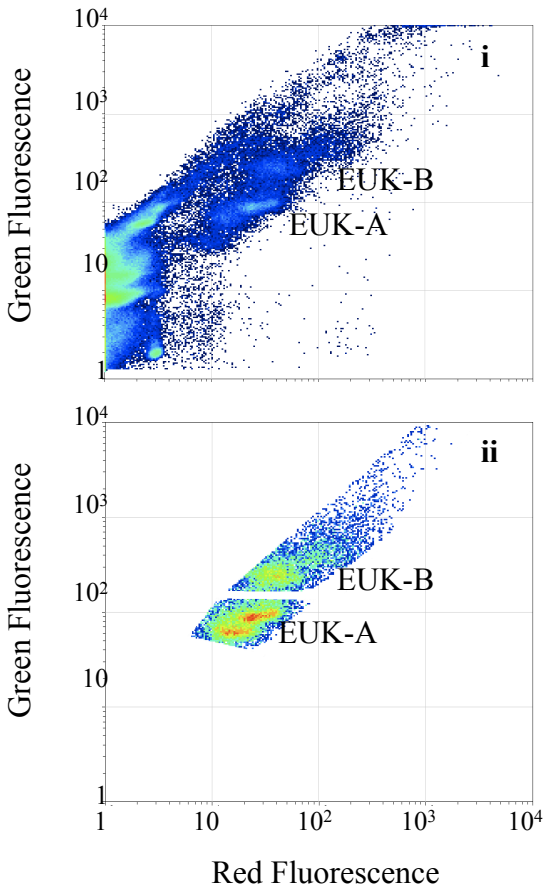

Supplementary Fig. 1. Characteristic flow cytometric signatures of SYBR Green I stained eukaryotic phytoplankton showing (i) the separation between photosynthetic eukaryotic groups Euk-A and Euk-B, respectively, and (ii) the Euk-A and Euk-B groups of cells sorted by flow cytometry.

Sequence	Accession number	Sequence	Accession number
AS2_50C19	AY702195	Biosope_UPW1_5m_C1	FJ649262
AS2_50C3	AY702193	Biosope_STB1_25m_C7	FJ649268
AS10_50C6	DQ013167	Biosope_STB1_25m_ D5	FJ649275
AS10_50C7	DQ013168	Biosope_STB1_25m_D6	FJ649276
AS10_50C3	DQ013166	Biosope_STB1_25m_E6	FJ649281
environmental clone OCS31	AF001655	Biosope_STB1_25m_E8	FJ649282
UC prymnesiophyte OM21	U32671	Biosope_STB1_25m_E10	FJ649284
Unidentified eukaryote OM270	U70723	Biosope_STB11_5m_E9	FJ649283
Isochrysis sp.	X75518	Biosope_STB11_5m_F1	FJ649287
Ochrosphaera neapolitana CCMP593	X80390	Biosope_STB11_5m_E12	FJ649286
UC prymnesiophyte DYF25	AY702172	Biosope_STB17_30m_F12	FJ649293
UC prymnesiophyte HE3	AY702175	Biosope_STB17_30m_G2	FJ649295
UC prymnesiophyte DYF45	AY702174	Biosope_STB17_30m_G9	FJ649301
Phaeocystis cordata RCC186	AY702142	Biosope_STB17_30m_G10	FJ649302
Emiliania huxleyi RCC192	AY702115	Biosope_STB17_30m_H4	FJ649308
Chrysochromulina acantha RCC339	AY702152	Biosope_STB17_30m_H9	FJ649313
coccoid prymnesiophyte RCC406	AY702162	Solas_16400_NF02	FJ797583
Imantonia rotunda RCC305	AY702150	Solas_16400_NF12	FJ797588
uncultured phototrophic eukaryote pT-411	AY095882	Solas_16400_NF03	FJ797584
Chrysochromulina polylepis	AF172719	Solas_16400_NH12	FJ797591
250304-21	EF052021	Solas_16400_NG09	FJ797590
250304-51	EF052048	Solas_16400_NG08	FJ797589
MAMA64-138	EF051997	Solas_16400_NF10	FJ797587
MAMA64-126	EF051987	Solas_16400_NF08	FJ797586
MAMA64-113	EF051975	Solas_16400_NF05	FJ797585
MC597-22	EF051786	Solas_16400_NE12	FJ797582
MC601-136	EF051927	Solas_16400_NE02	FJ797581
MC615-104	EF052171	Solas_16400_ND10	FJ797580
MC615-36	EF052110	Solas_16400_ND09	FJ797579
MC622-62	EF052222	*Dicrateria inornata* CCMP355	EF051750
MC622-16	EF052183	*Chrysochromulina simplex*	EF051754
MC622_72	EF052232	*Chrysochromulina throndsenii*	EF051755
MC622_58	EF052218	*Chrysochromulina campanulifera* UIO J10	EF051761
Biosope_MAR1_15m_M1	FJ649229	*Chrysochromulina leadbeateri*	EF051759
Biosope_MAR1_15m_M2	FJ649230	*Chrysochromulina cymbium*	EF051760
Biosope_MAR1_15m_M3	FJ649231	*Phaeocystis cordata*	EF051764
Biosope_MAR1_15m_M7	FJ649234	*Phaeocystis jahnii* B5	EF051765
Biosope_MAR1_15m_M8	FJ649235	*Platychrysis* sp.	AB196968
Biosope_MAR1_15m_M9	FJ649236	*Chrysochromulina* aff. *polylepsis* PLY200	EF051752
Biosope_MAR1_15m_M10	FJ649237	*Isochrysis* cf. *galbana* UIO Ryfylke	EF051757
Biosope_MAR1_15m_A4	FJ649244	*Chrysochromulina herdlensis* CCMP284	EF051749
Biosope_UPW1_5m_B4	FJ649254	*Chrysochromulina rotalis* UIO TH2	EF051756
Biosope_UPW1_5m_B12	FJ649261		

Supplementary Table 1. Genbank accession numbers of plastid 16S rRNA gene sequences presented in Fig. 6